Research Paper

Oval Cells Contribute to Fibrogenesis of Marginal Liver Grafts under Stepwise Regulation of Aldose Reductase and Notch Signaling

Xiao-Bing LIU[1], Chung-Mau LO[1, 5], Qiao CHENG[1], Kevin Tak-Pan NG[1], Yan SHAO[1], Chang-Xian LI[1], Sookja K CHUNG[2], Irene Oi Lin NG[3], Jun YU[4], Kwan MAN[1, 5 ✉]

1. Department of Surgery, The University of Hong Kong, Hong Kong SAR, and Collaborative Innovation Center for Diagnosis and Treatment of Infectious Diseases, China;
2. School of Biomedical Sciences, The University of Hong Kong, Hong Kong SAR, China;
3. Department of Pathology, The University of Hong Kong, Hong Kong SAR, China; State Key Laboratory for Liver Research, The University of Hong Kong, Hong Kong SAR, China;
4. Institute of Digestive Disease and The Department of Medicine and Therapeutics, State Key Laboratory of Digestive Disease, Li Ka Shing Institute of Health Sciences, The Chinese University of Hong Kong, Hong Kong SAR, China;
5. Shenzhen Institute of Research and Innovation, The University of Hong Kong, Hong Kong SAR, China.

✉ Corresponding author: Prof. Kwan Man; Address: L9-55, Department of Surgery, Lab Block, 21 Sassoon Road, Pokfulam, Hong Kong; Tel: 852-39179646; E-mail: kwanman@hku.hk; Fax: 852-39179634

Abstract

Background and Aims: Expanded donor criteria poses increased risk for late phase complications such as fibrosis that lead to graft dysfunction in liver transplantation. There remains a need to elucidate the precise mechanisms of post-transplant liver damage in order to improve the long-term outcomes of marginal liver grafts. In this study, we aimed to examine the role of oval cells in fibrogenic development of marginal liver grafts and explore the underlying mechanisms.

Methods: Using an orthotopic rat liver transplantation model and human post-transplant liver biopsy tissues, the dynamics of oval cells in marginal liver grafts was evaluated by the platform integrating immuno-labeling techniques and ultrastructure examination. Underlying mechanisms were further explored in oval cells and an Aldose reductase (AR) knockout mouse model simulating marginal graft injury.

Results: We demonstrated that activation of aldose reductase initiated oval cell proliferation in small-for-size fatty grafts during ductular reaction at the early phase after transplantation. These proliferative oval cells subsequently showed prevailing biliary differentiation and exhibited features of mesenchymal transition including dynamically co-expressing epithelial and mesenchymal markers, developing microstructures for extra-cellular matrix degradation (podosomes) or cell migration (filopodia and blebs), and acquiring the capacity in collagen production. Mechanistic studies further indicated that transition of oval cell-derived biliary cells toward mesenchymal phenotype ensued fibrogenesis in marginal grafts under the regulation of notch signaling pathway.

Conclusions: Oval cell activation and their subsequent lineage commitment contribute to post-transplant fibrogenesis of small-for-size fatty liver grafts. Interventions targeting oval cell dynamics may serve as potential strategies to refine current clinical management.

Key words: hepatic bipotent cells; small-for-size fatty graft injury; aldose reductase; notch signaling.

Introduction

With the ever increasing demand on liver transplantation, marginal liver grafts such as small-for-size and/or fatty grafts have been adopted to expand the liver donor pool in recent years. Yet it has been long noted that marginal liver grafts in living donor liver transplantation (LDLT) are more susceptible to insults such as ischemia reperfusion (I/R) injury and viral infection after transplantation

[1, 2], which result in worse graft function and survival [3, 4].

Post-transplant fibrosis is a common reason for late-phase graft dysfunction in liver transplantation [5, 6]. Increasing data have demonstrated the strong association between activation of hepatic bipotent progenitor cells (oval cells) and fibrogenesis [7, 8]. Some recent studies also suggested that oval cells may contribute to liver fibrosis by serving as a source of myofibroblasts [9, 10]. However, the direct participation of oval cells in liver graft fibrosis remains undefined, especially in terms of how oval cells are initiated and terminated into extracelluar matrix (ECM)-producing cells in marginal liver grafts.

Liver transplant procedure with its related ischemia/reperfusion (I/R) injury and the surgical trauma resulted in inflammation detrimental to allograft function [11]. Our recent study showed that Aldose reductase (AR), a polyol pathway enzyme traditionally believed to play essential roles in glucose metabolism and detoxification of a wide range of aldehydes, was a critical responsive gene to inflammation after liver transplantation [12] . Study from other research group also reported that AR affected the development of diet-induced liver steatosis [13]. Nevertheless, the cross-talk between AR and oval cells in fibrogenic development in marginal grafts has not been explored so far.

Epithelial-to-Mesenchymal transition (EMT) is a critical physio-pathological phenomenon observed either in embryonic development, fibrosis or cancer progression. In latest years, there has been increasing interest in the role of EMT in fibrogenesis during chronic liver diseases [7, 14-16]. Yet whether certain types of liver cells such as biliary cells are capable of undergoing EMT in liver injury remained controversial [16-19]. Meanwhile, morphological evidence supporting the presence of transition was scarce.

In this study, with an orthotopic rat liver transplantation model mimicking marginal graft injuries encountered in human living donor liver transplantation, we demonstrated that aldose reductase triggered oval cell proliferation during the early phase after transplantation. Following acquisition of biliary differentiation in the mid-late phase, these progenitor cells contributed to graft fibrogenesis via mesenchymal transition, which was regulated by notch signaling pathway.

Materials and Methods

Experimental design

The study consisted of three parts. In part I, post-transplant oval cell activation in marginal liver grafts was evaluated in an orthotopic rat liver transplantation model simulating clinical living donor liver transplantation. Then lineage commitment of oval cells as well as its association with fibrogenesis was examined in serially collected samples. In part II, the findings in the rat model were validated in human post-transplant liver biopsy specimens. In part III, the underlying mechanisms regulating oval cell activation and graft fibrosis were further explored in mouse models and oval cells *in vitro*.

Patients and clinical samples

Liver biopsy specimens from small-for-size fatty grafts (living donor liver transplantation) or whole normal grafts (deceased donor liver transplantation) were obtained from the department of pathology and the department of surgery, HKU from 2005 to 2012. To evaluate the extent of fatty change in the donor grafts, a small piece of liver tissue was removed from each donor graft in the operation theatre before transplantation by an experienced surgeon. Then the tissue was sent to the department of pathology for fatty change grading. The samples are usually categorized into 0 (no fatty change), 1 (mild, fatty change ≤10%), 2 (moderate, fatty change=11-30%) or 3 (severe, fatty change>30%). Post-transplantation liver biopsy samples were retrieved from the paraffin blocks in the Department of Pathology. All the biopsies were performed for clinical diagnostic purposes and no additional injury was incurred in the patients. The clinical research ethics of the current study have been approved by the Institutional Review Board (IRB) of The University of Hong Kong. Written informed consent was obtained from all patients recruited in the study. All the specimens were fixed in neutral formalin and then embedded in paraffin blocks.

Animal models and tissue collection

Animal care and surgical procedures were performed according to the University of Hong Kong Committee on the Use of Live Animals in Teaching and Research.

Orthotopic rat liver transplantation

Male Sprague Dawley rats (body weight: 250~300 g) were used as donors or recipients of liver transplantation. Fatty liver grafts in the donors were induced by feeding the rats with HFD (the HFD was a purified TestDiet 58G8 with 45% energy from fat, TestDiet, USA) for 2 weeks. Cirrhosis of recipients was induced by subcutaneous injection of 50% carbon tetrachloride diluted with olive oil at a dose of 0.2 mL per 100 g of body weight twice a week for 6 weeks [4].

To establish the orthotopic small-for-size liver transplantation model, nonarterialized liver

transplantation without venovenous bypass was performed. The median ratio of graft weight to recipient liver weight (graft-weight ratio) was 59% (range 55–67%). The grafts were stored in cold saline with a target cold ischemic time of 40 min. The anhepatic phase was 17~21 min.

Hepatic I/R injury and major hepatectomy in wild-type or AR knockout mice

Inbred male C57BL/6 (6~8 weeks old) mice were obtained from Laboratory Animal Unit, The University of Hong Kong. AR knockout mice of C57BL/6 background were obtained from Professor S.K. Chung (School of Biomedical Sciences, The University of Hong Kong). Fatty liver was induced in C57BL/6 and AR knockout mice by feeding HFD for 2 weeks and the fatty change was about 30% to 40%. All the mice were subjected to major hepatectomy and partial hepatic IRI to mimic the clinical situation. The branches of hepatic artery and portal vein to the right and triangle lobes were clamped for 45 minutes by microvessel clamp, followed by reperfusion (release of the clamp). Major hepatectomy of the left and caudate lobes was performed during ischemic period. The mice were sacrificed at day 2, 4 and 7 after reperfusion [12, 20].

Liver tissues from animals were collected at different time points and stored at -80°C or fixed in neutral formalin.

Morphological studies by light and electron microscopy

Histological alteration in liver tissues was evaluated under light microscopy after hematoxylin and eosin staining or Masson's trichrome staining. For electron microscopy examination, liver tissues of 1 mm cubes in size were fixed in 2.5% glutaraldehyde overnight and processed to sectioning as reported previously [1]. After staining with uranyl acetate and lead citrate, the sections were examined under a transmission electron microscope (Philips EM208S, Eindhoven, Holland).

Cell culture and differentiation induction

Murine oval cell line (PIL2) was cultured and maintained as previously reported [2]. To induce biliary differentiation, oval cells were collected and re-suspended in culture medium. After mixing with matrigel, the cells were gently spread over the surface of filter insert and incubated at 37°C for 30 min. Conditional medium supplemented with epidermal growth factor (EGF, 20 µg/ml), hepatocytes growth factor (HGF, 10 ng/ml) and keratinocyte (KGF, 50 ng/ml) was then applied at both sides of the insert.

Transfection of aldose reductase plasmid

To over-express aldose reductase (AR) in oval cells, AR expressing plasmid was constructed by cloning a full-length cDNA of mouse AR gene (GI:NM_009658) into pcDNA3.1(+) vector. Then the oval cells were transfected with pcDNA3.1 (+)-AR plasmids (2 µg/ml, 4 µg/ml or 8 µg/ml) by a microelectroporator (NeonTM Transfection System, Life science, USA). Empty pcDNA3.1(+) was used as a negative control. The transfection efficiency was monitored by pcDNA6.2/emGFP plasmid (Life science, USA). The cells were collected 48 hr after transfection for further analysis.

Cell cycle analysis

Oval cells in six-well plates were harvested after exposure to Zopolrestat (12.5 µM) for 48 hours. After incubation with 1 ml propidium iodide (PI) (50 µg/ml) and 50 µl RNase A (100 µg/ml) at 37°C for 30 min, cell cycle was analyzed using BD FACSCalibur flow cytometer.

Cell proliferation Assay

Oval cell proliferation after AR plasmid transfection or Zopolrestat supplement was performed in 96-well plates using Cell Titer 96® AQueous One Solution Cell Proliferation Assay (Promega, Madison. WI, USA) as instructed by the manufacturer.

Scratch assay

Oval cells grown in monolayer in 12-well plates were artificially injured by scratching across the plate with a pipette tip. The wells were washed and supplemented with serum-free medium containing either TGFβ-1 (5 ng/ml) or TGFβ-1(5 ng/ml) in combination with dibenzazepine (5 nM). After 16 hours, images of the scratched areas under each condition were photographed.

Quantitative real-time PCR

Real-time PCR analysis was carried out using SYBR Green PCR Master Mix (Applied Biosystems) as reported previously [3]. The sequences of sense and antisense primers were summarized in Table S1. Expression levels of genes were determined after normalizing to internal control 18S.

Immuno-histo(cyto)chemistry

Immunostaining was performed as reported previously [20]. The primary antibodies used were as indicated in Table S2. For immuno-fluorescent staining, goat anti-rabbit (Alexa Fluor® 488) or donkey anti-mouse (Alexa Flour® 594) secondary antibodies were applied. The signals were then analyzed by a confocal microscope (LSM710, Carl

Zeiss) with laser lines at the wavelength of 488 nm and 561 nm respectively. Signal of DAPI was detected with the laser line at the wavelength of 405 nm.

Cells inside matrigel were fixed in 4% paraformaldehyde and permeabilized with 0.5% triton X-100. Then immunofluorescent staining was performed with primary antibodies overnight at 4°C and subsequently with second antibodies at room temperature for 1 hour. The nuclei were counterstained with DAPI and images were photographed with a fluorescent microscopy (Nikon, eclipse 80i). The integrated intensity of immunostaining signals was quantified by software ImageJ.

Immuno-FISH

Immunofluorescent labeling was performed using a streptavidin method with primary antibody against CK19 and goat anti-rabbit Alexa Fluor® 488 secondary antibody. Then the slides were hybridized with the probe set for collagen type I, alpha 1 mRNA (Stellaris) as instructed by the manufacturer. Briefly, the slide was incubated with hybridization buffer containing probe (125 nM) at 37°C for 6 hours. Then the nuclear was counterstained with DAPI and the signals were examined under a fluorescent microscope.

Western blot analysis

Cell lysates were separated by SDS-PAGE and transferred to PVDF membranes. After incubation with primary and secondary antibodies, signal was developed and band intensities were quantified by software ImageJ.

Statistics

All data were expressed as mean ± SD. Statistical analysis was performed using Student's t test. All analysis was conducted using SPSS software. Differences with $p < 0.05$ were considered to be statistically significant.

Results

Proliferative oval cells exhibited dominant biliary differentiation in small-for-size fatty liver graft

Liver steatosis, together with other insults may impair hepatocyte regeneration and lead to activation of bipotent hepatic progenitor cells in liver diseases. To assess liver regeneration in the small-for-size fatty grafts after transplantation, immunostaining with Ki-67 was performed on rat liver tissues. Compared to whole normal grafts, hepatocytes in small-for-size fatty graft demonstrated a lower proliferation index at Day 2 and Day 4 (Figure 1A, B), which indicated that

the regenerative capacity of hepatocytes was suppressed.

On the other hand, starting from Day 4, prominent ductular proliferation in the portal–parenchymal interphase of small-for-size fatty grafts was identified by morphological examination on liver tissue sections. High magnification of the tubular structure revealed small singular cells with oval nucleus and small cytoplasm closely resembling progenitor cells (Figure S1). Histochemically staining demonstrated that these cells were strongly stained with hepatic oval cell marker (Ov6) on day 7 and day14 (Figure 1C) after transplantation. In whole normal grafts, the expression of Ov6, however, were weakly detectable in periportal biliary cells. The integrated intensity of Ov6 between these 2 groups was significantly different (Figure 1D). Activation of oval cells was also verified in human small-for-size fatty grafts (Figure 1E). Furthermore, amid the expanded small atypical tubular structures, an increase of well-formed ductules with defined lumina was identified on day 7 after transplantation. Because distribution of E-cadherin was used to distinguish oval cells from biliary cells [21], we also assessed the expression pattern of this marker in the liver tissues to confirm the presence of oval cells. As shown in Figure S2, strong immunoreactivity was observed in the ductular structures of small-for-size fatty grafts and most positive cells hold E-cadherin on the whole cell membrane (both basolateral and apical sides). In contrast, the ductular cells in the whole normal grafts showed weak immunoreactivity for E-cadherin only on their basolateral membrane. Immuno-fluorescent staining demonstrated that the ductular cells co-expressed Ov6 and E-cadherin (Figure 1F) instead of hepatocyte marker albumin (data not shown). These findings implied that hepatic oval cell compartment was boosted when there was insufficient proliferation of hepatocytes in small-for-size fatty grafts. And these oval cells differentiated mainly along biliary lineage during tissue repair.

Activation of aldose reductase triggered oval cell proliferation

Our recent study reported that Aldose reductase (AR) was a major player in inflammation induced graft injury [12]. Here we found that mRNA level of AR was remarkably augmented in the small-for-size fatty grafts on day 2, day 7, day 14 after transplantation compared to that in whole normal grafts (Figure S3). Increased expression of AR protein in the proliferative ductules was also verified by immunohistochemical staining (both in rat and human) (Figure 2A).
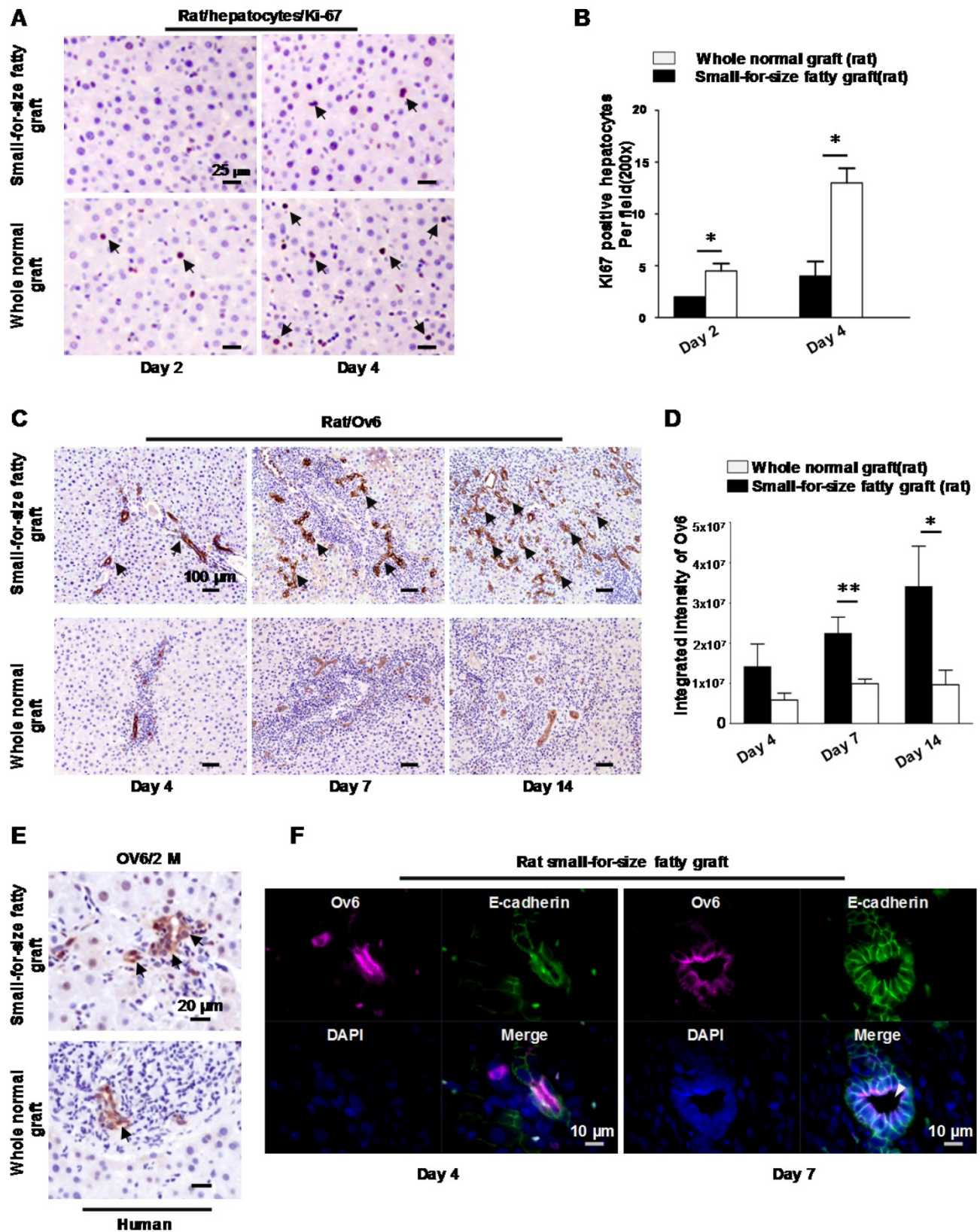
Figure 1. Hepatic progenitor cells (oval cells) proliferated in small-for-size fatty grafts and exhibited dominant biliary differentiation. (A) Suppressed hepatocyte regeneration in small-for-size fatty grafts (Ki-67 staining, arrows) post-transplantation (n=6). **(B)** Statistical analysis of Ki-67 positive hepatocytes under microscopic examination. **(C)** Enhanced expression of Ov6 (hepatic progenitor cell marker, arrows) in the proliferative ductules of small-for-size fatty grafts (n=6). **(D)** Integrated intensity of Ov6 expression. **(E)** Increased proliferation of oval cells (Ov6 staining, arrows) in human small-for-size fatty graft. **(F)** Co-localization of Ov6 and E-cadherin (day 4, day 7) and development of defined lumina (arrowhead) on day 7 in the ductules of rat small-for-size fatty grafts. * $p<0.05$; ** $p<0.01$.
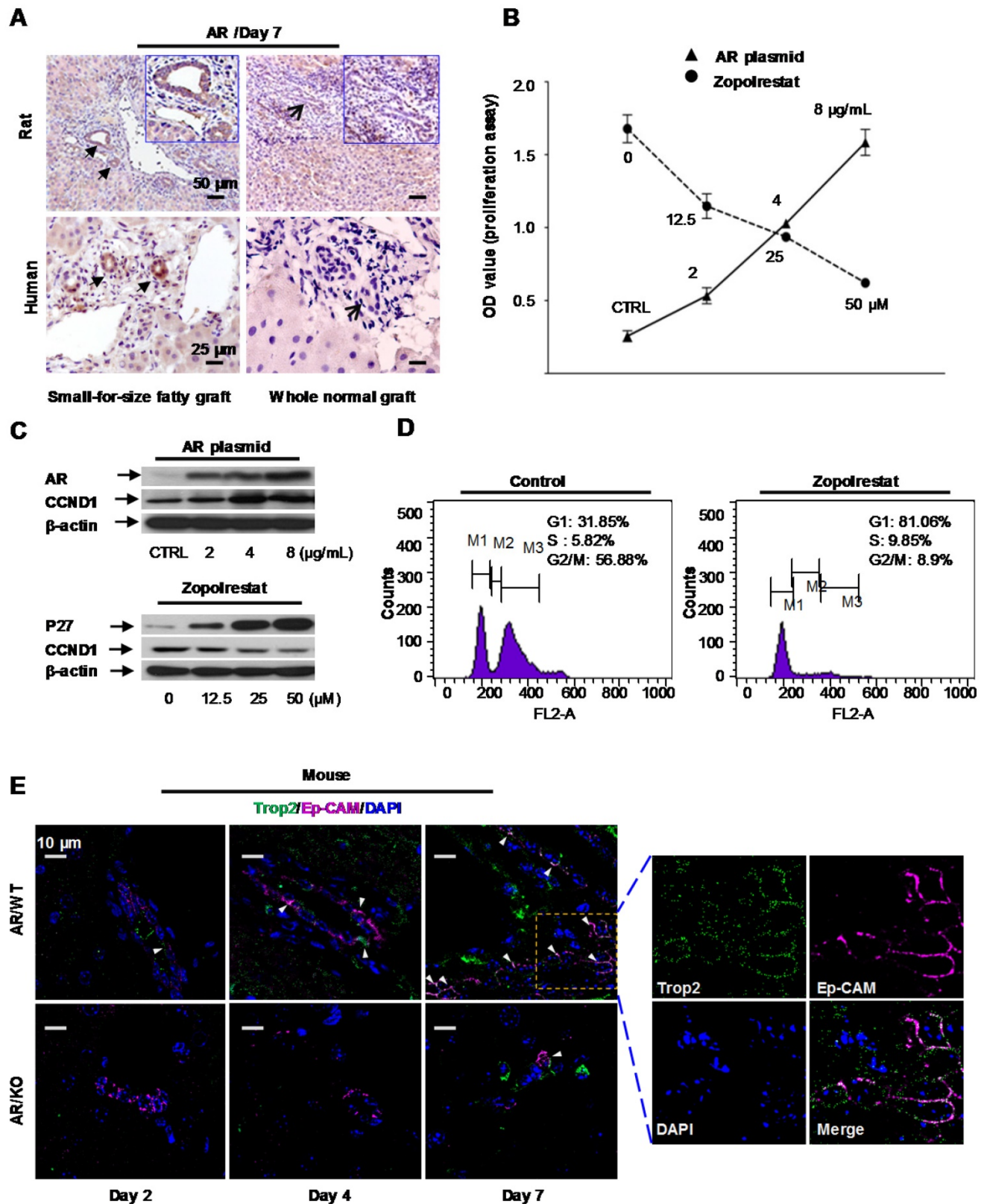
Figure 2. Aldose reductase (AR) regulated oval cell proliferation. (**A**) Over-expression of aldose reductase in proliferative biliary cells of rat or human small-for-size fatty grafts (the arrows indicated the biliary cells). (**B**) Effect of AR plasmid (solid line) and AR inhibitor Zopolrestat (dashed line) on the growth of oval cells. (mean ± SD, n=3, p<0.05) (**C**) Effect of AR plasmid and Zopolrestat on the expression of cell cycle related genes. (**D**) Zopolrestat blocked cell cycle of oval cells at G1/S. (**E**) In AR wild type mouse model simulating small-for-size fatty graft injury, activated oval cells (Trop2, green color) co-expressed Ep-CAM (magenta color) (arrows) (n=6). In contrast, fewer oval cells were observed in AR knockout mouse model.

To elucidate the functional impact of AR, pcDNA 3.1(+) vector over-expressing Aldose reductase gene was transfected into murine oval cells in vitro. We found proliferation of oval cells was enhanced after AR plasmid transfection (Figure 2B, solid line). Analysis at the protein level showed that augmentation of AR was accompanied with increased expression of cell cycle regulatory gene, such as CyclinD1(CCND1) (Figure 2C, upper panel). Consistent with this finding, Zopolrestat (a potent inhibitor to knock down AR activity) (Sigma-Aldrich, USA) suppressed the proliferation of oval cells proportional to the administered doses (Figure 2B, dashed line), and resulted in concurrent over-expression of P27 and down-regulation of CyclinD1 (Figure 2C, lower panel). Flow cytometry analysis further demonstrated that proliferation of oval cells was blocked at G1/S phase after addition of Zopolrestat (Figure 2D).

Post-transplant small-for-size fatty liver graft injury can be simulated in mice by ischemia/reperfusion (I/R) induction followed by major hepatectomy. In this study, to elucidate the role of aldose reductase in marginal graft injury, we introduced I/R and hepatectomy to AR wild type or knockout mice with diet-induced fatty livers as previously reported [12]. Immunostaining with mouse oval cell marker Trop2 [22] demonstrated that proliferation of oval cells was significantly blocked in AR knockout mice at the early-middle phases (day 2, day 4, day 7) after injury (I/R + major hepatectomy) (Figure 2E, Figure S4). It suggested that AR directly triggered oval cell proliferation in liver injury mimicking small-for-size fatty graft damage.

Oval cell-derived biliary cells demonstrated dynamic co-localization of epithelial and mesenchymal markers

To evaluate whether EMT plays a role in post-transplant fibrosis in small-for-size fatty grafts, we firstly assessed the expression of epithelial (CK19) and mesenchymal (Vimentin) markers in the liver grafts. Immuno-fluorescent staining demonstrated that the proliferative ductules showed immunoreactivity for both CK19 and Vimentin on day 7 (middle phase) or day 14 (late phase) (Figure 3A). 3D re-construction of Z stacking images verified that these fluorescently labeled cells shared identical rather than proximal location (Figure 3B). Additionally, co-localization analysis indicated that signal from CK19 (green) co-localized with signal from Vimentin (magenta) to a moderate (day 7) or less than moderate (day 14) degree (Table S3). To evaluate the dynamics of CK19 and Vimentin in proliferative ductules, expression of these two proteins was also assessed in serial sections. As indicated in Figure 3C and Figure S5, immunoreactivity of the proliferative ductules for CK19 declined while Vimentin augmented after transplantation from day 7 to day 14. In human transplants, a dynamic co-localization of CK19 (decrease) with Vimentin (increase) in biliary cells (Figure 3D and Figure S6) was also confirmed in marginal grafts (6 or 11 months).

Altogether, we found that proliferative biliary cells in small-for-size fatty liver grafts dynamically co-expressed epithelial (loss of expression) and mesenchymal (increase of expression) markers. This signaled that epithelial-to-mesenchymal transition (EMT) was initiated in these oval cell-derived biliary cells in response to post-transplant injury in marginal liver grafts.

## Oval cell-derived biliary cells developed migration and transition microstructures

In this study, with the help of transmitting electron microscopy (TEM), we revealed 3 migration-associated microstructures, including podosomes, filopodia and blebs in marginal liver grafts on day 14 after transplantation. Podosomes appeared as small plasma-membrane extensions on the basal side of transitional biliary cells (Figure 4A). In line with this structure, accumulation of podosome-associated protein Cortactin (Figure 4B, upper left panel) in biliary cells was verified by immunostaining. Additionally, inside these podosomes, a large amount of lysosome-like bodies were identified (Figure 4A, magnified image), which was in accordance with concurrent increased expression of matrix-degrading proteases such as Mmp14 (MT1-MMP) (Figure 4B, upper right panel) in the proliferative biliary cells. This suggested a role of podosomes in degrading extracellular matrix (ECM). Filopodia were protrusions extending from the basal or lateral sides of the elongated biliary cells and contacting with passing non-biliary cells or extracellular collagen fibers (Figure 4C). Consistent with this morphological finding, over-expression of Arpc2 (an important protein in filopodia formation) as well as its co-localization with Mmp9 in biliary cells was observed (Figure 4D). Furthermore, we identified that part of plasma membrane separated from the cellular cortex to form blebs in the leading edge of elongated biliary cells. This microstructure grew into spherical protrusions contacting with passing non-biliary cells (Figure 4E).

We also identified several lines of evidence indicating mesenchymal transition (EMT) of biliary cells in small-for-size fatty grafts such as spindle change in shape (Figure S7, left upper panel), partially or completely disappearance of cellular junctions

(Figure S7, right upper panel), basement membrane damage (Figure S7, left lower panel) and increased microfilaments in the cytosol (Figure S7, middle and right lower panels).

In line with the features suggested by TEM analysis in rat model, immunostaining with laminin revealed discontinuity of basement membrane surrounding the biliary cells (Figure 4F) in human marginal grafts. This served as additional evidence that the biliary cells may enter the surrounding matrix through the collapsed basement membrane in small-for-size fatty liver grafts.
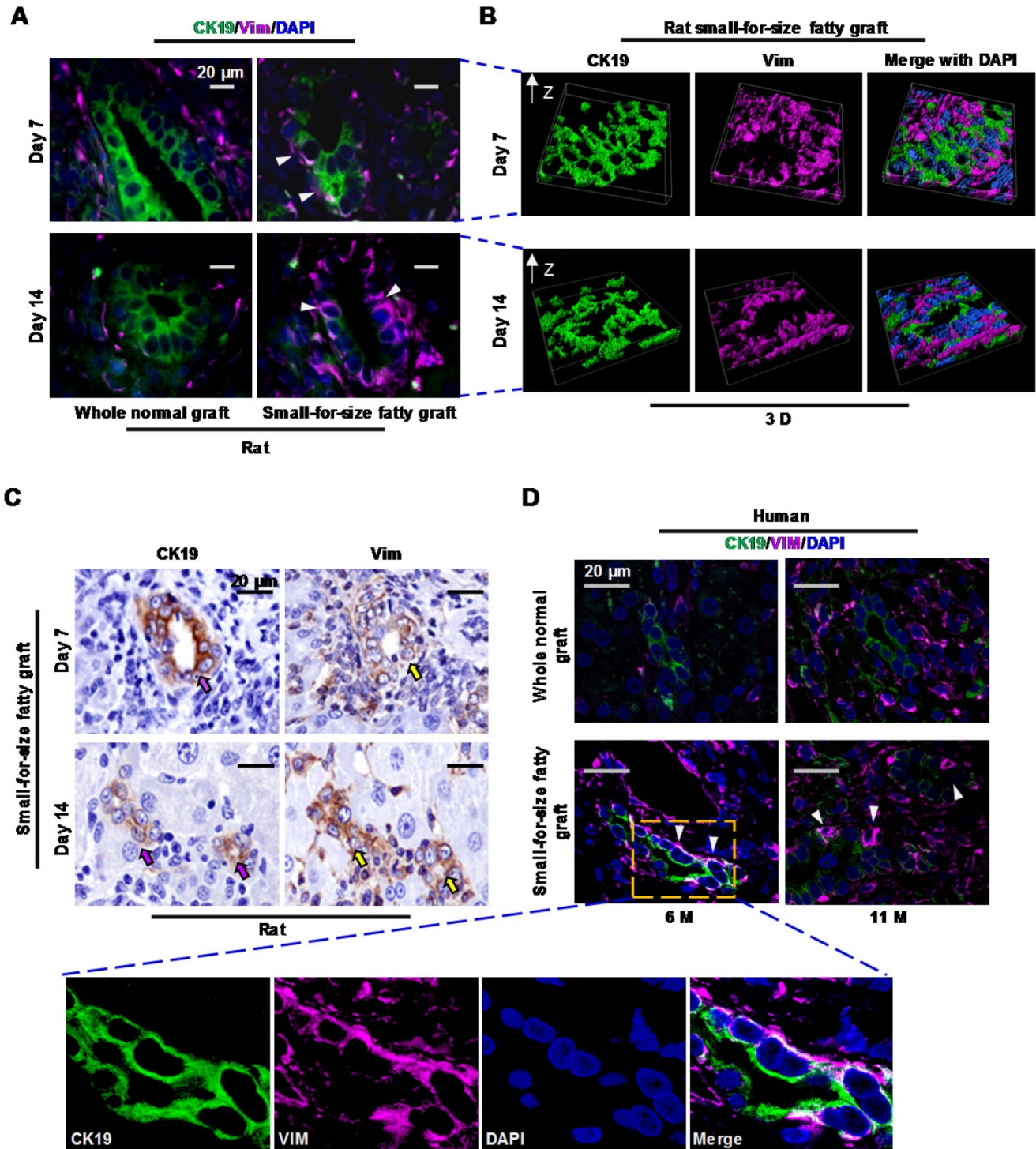
Figure 3. Proliferative biliary cells in small-for-size fatty graft dynamically co-expressed CK19 and Vimentin. (**A**) Co-localization of epithelial (CK19) and mesenchymal (Vimentin) markers in reactive ductules (arrowheads) of post-transplant small-for-size fatty grafts. (**B**) Co-localization of CK19 and Vimentin in small-for-size fatty graft revealed by 3D reconstruction (z-stacking under confocal microscopy). (**C**) Dynamic expression of CK19 (decreased, pink arrows) and Vimentin (increased, yellow arrows) in the proliferative ductules of small-for-size fatty grafts (serial sections). (**D**) Dynamic co-localization of CK19 and Vimentin in the proliferative ductules (arrowheads) of human small-for-size fatty graft at 6 and 11 months post-transplantation.
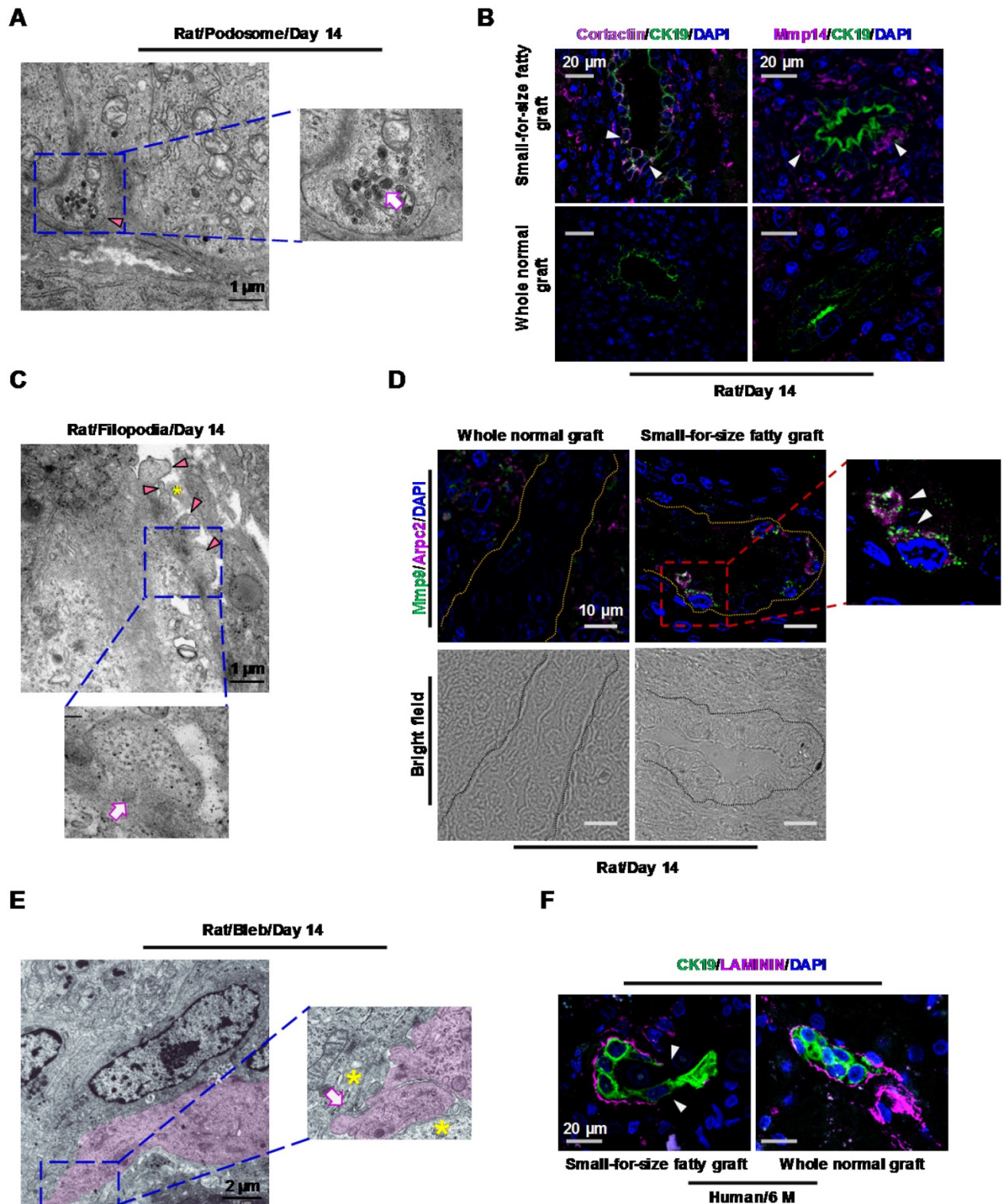
Figure 4. Transitional biliary cells in small-for-size fatty graft showed features of collagen remodeling and migration. (**A**) Podosome (arrowhead) with increased lysosome-like structures (magnified image, arrow) in the cytoplasm of transitional biliary cells (day 14). (**B**) Accumulation of podosome-associated protein Cortactin (magenta color) was accompanied with concurrent augmentation of matrix-degrading protease Mmp14 (magenta color) in biliary cells (arrowheads). (**C**) Filopodia protrusions (arrowheads) extended from the basal or lateral sides of transitional biliary cells and contacted adjacent extracellular matrix (asterisk). Microfilaments (magnified image, arrow) parallel to cell membrane were identified in the cytosol near protrusions. (**D**) Co-localization of Arpc2 (a protein for filopodia formation, arrowheads) and Mmp9 in biliary tubules (bright field, circled by dashed line) in small-for-size fatty graft (day 14). (**E**) In the leading edge of transitional cells (pink color), membrane blebs formed (magnified image, arrow) and contacted with passing non-biliary cells (magnified image, asterisks). (**F**) Discontinuity of base membrane (Laminin staining, arrowheads) surrounding biliary cells in post-transplant human small-for-size fatty graft (6 month).

Taken together, these data indicated that transition of biliary cells toward mesenchymal phenotype took place in small-for-size fatty graft. And during the process of transition, the biliary cells not only acquired the ability to remodel the collagen underneath but also alternatively adopted either filopodia-driven or blebbing motions to migrate into the surrounding tissue.

Transitional biliary cells acquired the ability of collagen synthesis

To assess whether these transitional biliary cells gained the ability to produce collagenous matrix, we examined the mRNA level of Pro-collagen I alpha 1 in the rat model. Analysis with in situ hybridization demonstrated that the proliferative ductular cells in small-for-size fatty grafts over-expressed Pro-collagen I alpha 1 mRNA, and this elevation was most prominent on day 14 after transplantation (Figure 5A, upper panels and the lower left panel). Additionally, we identified collagen deposition in the extracellular matrix surrounding proliferative ductules in late-phase graft (Day 14) (Figure 5B, upper panel), which served as the early trait of fibrotic development. Collectively, the findings suggested that the morphological alteration of EMT in biliary cells was accompanied with enhanced capacity in collagen production.

Notch signaling contributed to fibrogenesis via regulating EMT in biliary-differentiated oval cells

To explore the impact of notch signaling in fibrogenesis in small-for-size fatty grafts, the expression levels of Notch receptors 1~4 were assessed in either rat or human grafts which demonstrated features of EMT.

In the rat model, we found compared with whole normal grafts there was a significant increase of Notch 2 receptor mRNA in small-for-size fatty grafts (Figure 6A) which was accompanied with a rise of TGFβ-1 (Figure S8). Meanwhile, biliary cells in small-for-size fatty grafts showed prominent immuno-reactivity for Notch 2 (Figure 6B, left panel) and notch signaling effector Hes-1 (Figure 6C, left panel) on day 7 and day 14 after transplantation. In contrast, only very low level of Notch 2 was detected in the whole normal graft (Figure 6B, right panel). Additionally, increased level of Jag-1, which is a notch receptor ligand, was also observed in stromal cells surrounding the proliferative ductules in small-for-size fatty grafts (Figure 6C, right panel). Consistent with these findings, we confirmed the augmented expression of Notch 2 receptor in biliary cells of human small-for-size fatty grafts at 6 months post-transplantation (Figure 6D).
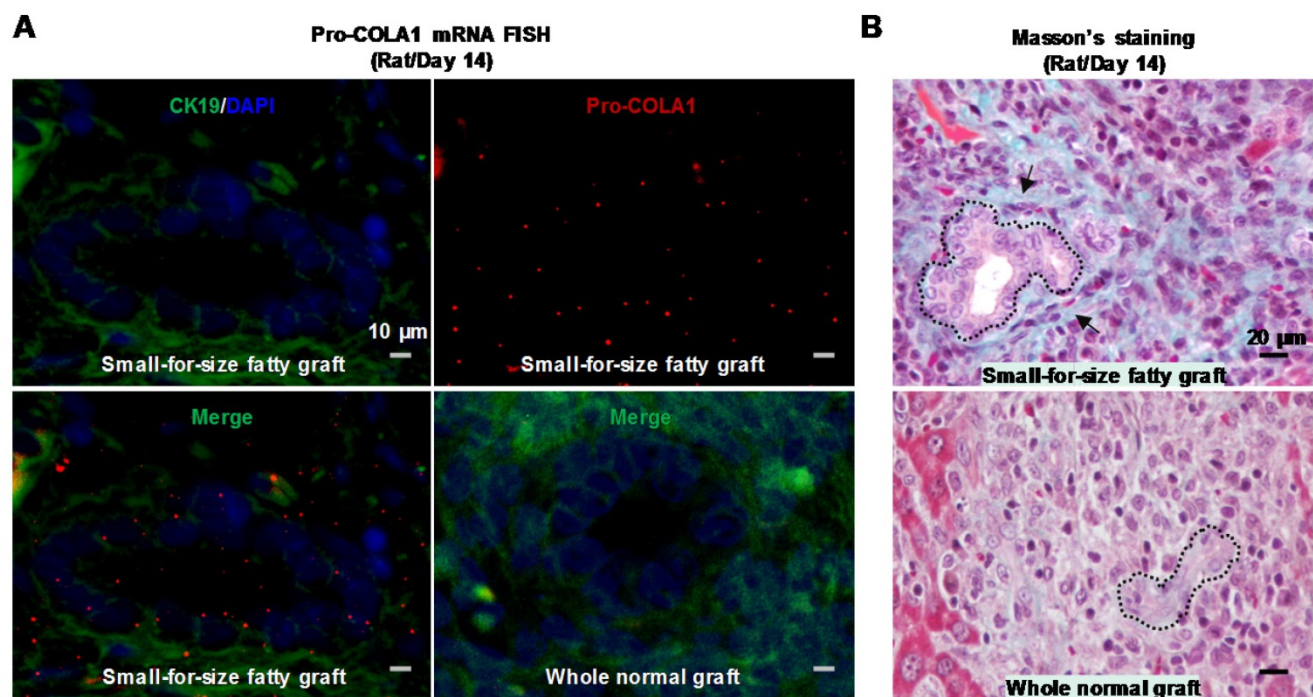
Figure 5. Biliary cells in small-for-size fatty graft showed collagen-producing capacity. Prominent expression of Pro-collagen I alpha 1 mRNA was identified in the biliary cells of small-for-size fatty grafts (A, upper panels and lower left panel; green color, CK19; red color, pro-collagen I α 1) (In situ hybridization, day 14). In contrast, signals of procollagen I α 1 were not detectable in the whole normal grafts (A, lower right panel). Masson's trichrome staining revealed collagen deposition (B, upper panel, arrows) surrounding the proliferative ductules of small-for-size fatty grafts (outlined by dashed lines, day 14).
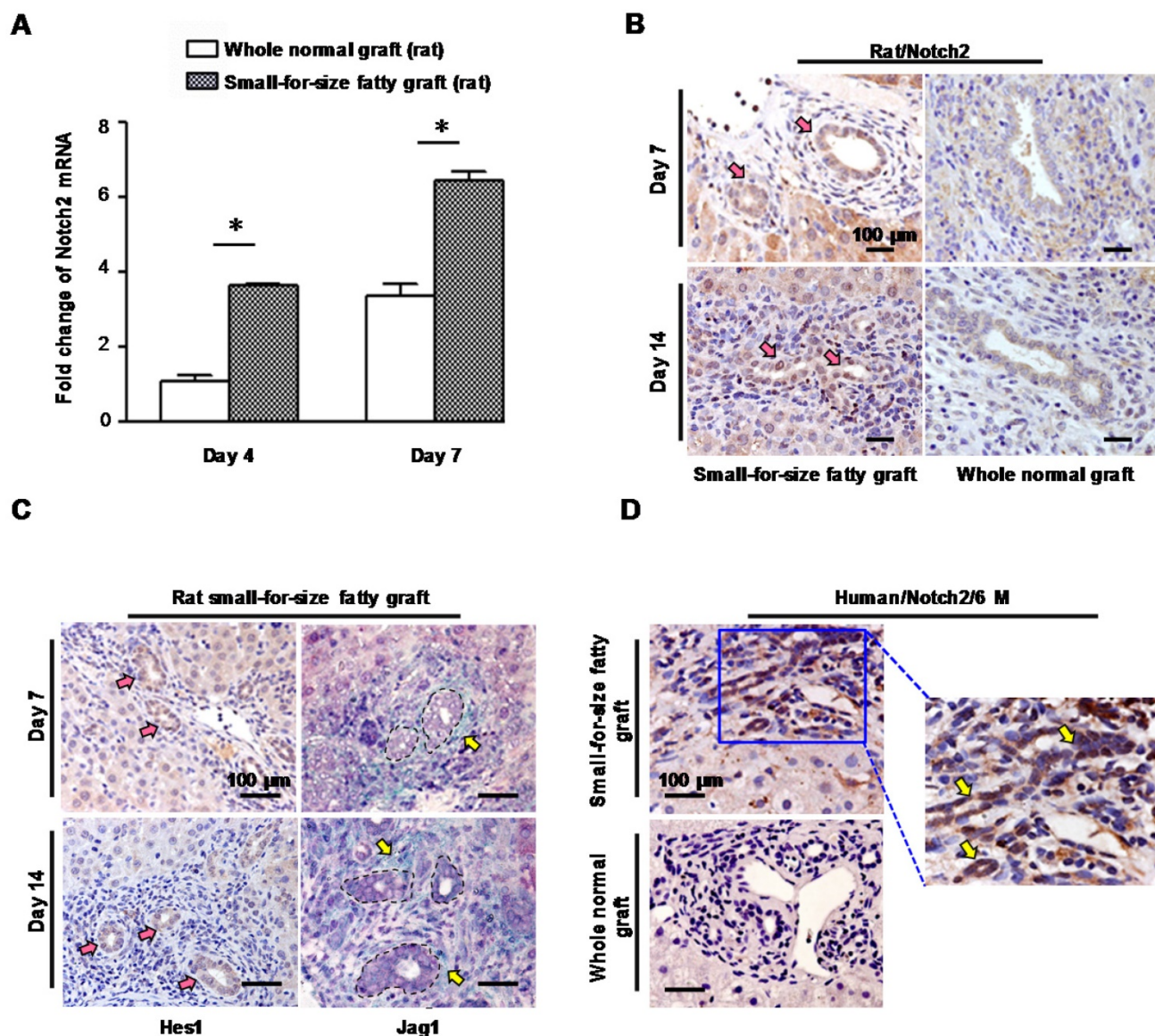
Figure 6. Notch signaling was activated in small-for-size fatty graft. (**A**) Increased mRNA level of Notch 2 in small-for-size fatty graft (rat, mean ± SD, n=6). ∗ p<0.05. (**B**) Over-expression of Notch 2 (pink arrows, DAB) in biliary cells of small-for-size fatty graft (rat) on day 7, day 14 post-transplantation in contrast to the whole normal graft (rat). (**C**) Up-regulation of Hes-1 (pink arrows, DAB) in biliary cells of small-for-size fatty graft was accompanied with an increase of Jag-1 (yellow arrows, Emerald) in adjacent stromal cells (biliary cells were circled inside dashed lines). (**D**) Increased Notch 2 expression (DAB, arrows) in biliary cells of post-transplant human small-for-size fatty graft (6 months) compared with that of the whole normal graft. Abbreviation: DAB, 3,3'-Diaminobenzidine.

To further evaluate the interaction between notch signaling and EMT in fibrogenesis, murine oval cells with biliary differentiation (Figure 7A, B) were exposed to γ-secretase inhibitor dibenzazepine (DBZ, a notch signaling inhibitor, Calbiochem, USA) with or without the presence of TGFβ-1 for 4 days.

We found TGFβ-1 augmented the levels of Notch 2 receptor as well as notch signaling effector Hes-1 (Figure 7C). And this was accompanied with altered expression of EMT (CK7, CK19, E-cadherin and SMA) and fibrogenic markers (Fibronectin, Collagen I α1) (Figure 7D).

Furthermore, we identified that inhibition of notch signaling with γ-secretase inhibitor dibenzazepine attenuated the mesenchymal transition of biliary-differentiated oval cells (Figure 7E, F). Consistently, scratch assay indicated that increased cellular mobility induced by TGFβ-1 was also suppressed by dibenzazepine (Figure S9). Meanwhile, supplement of dibenzazepine resulted in a paralleled decrease in fibrogenic markers such as Collagen I α1 and Fibronectin in these cells (Figure 7E).

Taken together, our data both in vivo and in vitro demonstrated that notch signaling pathway, especially notch 2 receptor contributed to fibrogenesis by regulating the mesenchymal transition of oval cell-derived biliary cells in the presence of TGFβ-1.
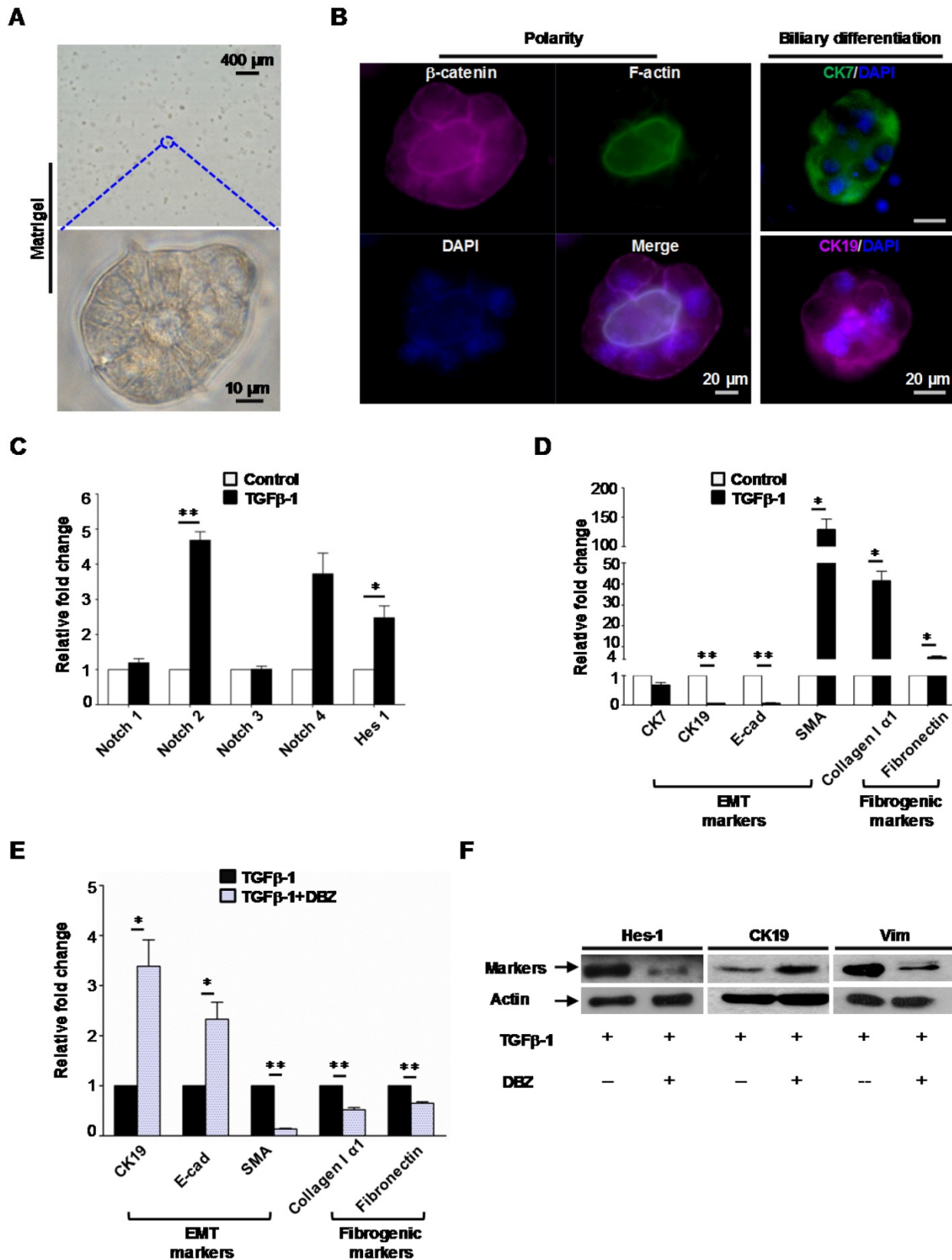
Figure 7. Notch signaling modulated mesenchymal transition and fibrogenesis of biliary-differentiated oval cells. (**A**) Oval cells formed acinus structures inside the matrigel after 4 days of induction. (**B**) Acinus polarity and biliary differentiation were revealed by immunofluorescent staining. (**C**) Augmented mRNA levels of Notch 2 and effector Hes-1 in biliary-differentiated oval cells after addition of TGFβ-1. (**D**) mRNA levels of epithelial (CK7, CK19, E-cadherin), mesenchymal (SMA) and fibrogenic (Collagen I alpha 1, Fibronectin) markers in biliary-differentiated oval cells with or without the presence of TGFβ-1. (**E**) Addition of γ-secretase inhibitor dibenzazepine (DBZ, 5 nM) mitigated the alteration of epithelial/mesenchymal markers and fibrogenic markers induced by TGFβ-1. (**F**) Representative epithelial/mesenchymal markers attenuated by DBZ in the presence of TGFβ-1(western blot). Data represent the mean ± SD (n=3) and are representative of at least 2 independent experiments in duplicate. * $p<0.05$, ** $p<0.01$.

Discussion

In the present study, we uncovered for the first time the mechanism which initiated oval cell proliferation during ductular reaction in small-for-size fatty grafts after transplantation. In both rat liver transplantation model and human post-transplant grafts, the proliferative oval cells in small-for-size fatty grafts over-expressed Aldose reductase (AR). In AR knockout mice simulating small-for-size fatty graft injury, we identified that loss of AR resulted in decreased oval cell expansion. In vitro study with oval cell line further confirmed that interference with AR plasmid or AR inhibitor influenced cellular proliferation and/or cell cycle. These data confirmed the regulatory role of AR in post-transplant oval cell proliferation in marginal grafts. Our observation was supported by recent emerging evidence which has extended AR's function to cell growth. For instance, Tammali et al. reported that AR-catalyzed reaction products of GS-aldehydes increased mitogenicity in colon cancer cells via activating NF-κB pathway [23]. Together with our recent findings [12], these results suggested that inhibition of AR may serve as an ideal strategy to prevent both inflammation and abnormal progenitor cell expansion in marginal grafts after transplantation.

Whether EMT participates in organ fibrosis remains highly controversial, especially in the field of hepatology [7, 14, 16-18]. Either difference in disease models or absence of direct evidence for transition has been suggested as the reasons for the discrepancies among studies. In this study, we examined EMT in the small-for-size fatty grafts of an orthotopic rat liver transplantation model. This model differed from other animal models in that liver cirrhosis was induced in the recipient rats before transplantation. Hence, it served as an ideal platform to simulate clinical setting as cirrhosis develops in a large number of patients before they receive liver transplantation. In this model, in addition to morphological evidence of mesenchymal transition, we discovered for the first time characteristic microstructures indicating participation of biliary cells in extracellular matrix remodeling (podosomes with electron dense lysosomes) as well as their cross beyond basement membrane (filopodia-like protrusions or membrane blebs).

Podosomes are unique adhesions that assemble early during cell adhesion to substrate. Morphologically, they appear as small plasma-membrane extensions 0.5~2 μm in width and depth [24-26]. Emerging evidence in recent years revealed that mature podosomes recruited multiple degrading proteases such as MMP9, MT1-MMP to degrade ECM and facilitate cell migration [27, 28]. In this study, we identified that existence of podosome-like protrusion on the basal side of biliary cells in small-for-size fatty grafts was accompanied with concurrent over-expression of proteins essential for podosome structure (Cortactin) and function (MT1-MMP). Furthermore, it is worth noting that we observed increased electron-dense lysosomes in podosome-like protrusions, which are rarely seen in normal biliary cells. Early studies have suggested that migrating endothelial cells dissolved extracellular collagen by a consecutive process of collagenase secretion, subsequent phagocytosis of collapsed fibers and final degradation in lysosomes [27-29]. In this study, we did not observe the engulfment of collagen fibrils by biliary cells partly because this process may be very transient. However, together with the massive destruction of basement membrane underneath podosome-like protrusions, these lines of evidence showed that the biliary cells acquired the ability to remodel the extracellular matrix and facilitate cellular movement beyond basement membrane. Further confirmation on the function of podosomes with immunoelectron microscopy labeling technique may be highly warranted in future studies. Filopodia-like protrusions and membrane blebs are microstructures [30-32] different in composition. Though the function of these microstructures remains largely unknown, an increasing number of recent studies suggested that either filopodia-driven movement or blebbing migration are important motility mechanisms in 3D environment. In this study, we identified in transitional biliary cells actin-rich filopodia or blebs in the leading edge went beyond the basement membrane and contacted interdigitally with surrounding non-biliary cells and/or collagen fibers. These data indicated that transitional biliary cells in small-for-size fatty grafts can migrate through ECM by adopting different movement modes. To our knowledge, this is the first study to report the existence of filopodia, blebs and podosome-like structures in epithelial cells. These data provided the direct evidence that proliferative biliary cells in marginal liver grafts were transformed to acquire the key features of mesenchymal cells, namely the capacity of remodeling ECM and migration.

Fibrosis is one potential outcome of EMT in tissue repair. Several studies have reported the expression levels of notch family members (such as Notch 3, Hes-1, Jag-1) in liver fibrosis models [33]. Yet the role of notch signaling in fibrogenesis of marginal liver grafts remains unclear. Herein we observed small-for-size fatty grafts with EMT features exhibited Notch 2 over-expression after transplantation. Meanwhile, we identified that TGFβ-1 induced EMT

and fibrogenesis via Notch 2 activation in biliary-differentiated oval cells in vitro, and blockade of notch pathway with notch inhibitor reversed the effect of TGFβ-1. Though it is difficult to dissect individual pathway in vivo for research purpose, our findings indicated that notch signaling integrated with TGFβ-1 to orchestrate fibrogenic activity of proliferative biliary cells by manipulating EMT. In combination with the aforementioned evidence of Pro-collagen α1(I) mRNA production in biliary cells and collagen accumulation in matrix surrounding biliary ductules, we suggested that in addition to other cell types such as hepatic stellate cells (HSCs), biliary cells reprogrammed in EMT constitute one source of liver fibrogenesis. And the new sights into the role of Notch 2 receptor in small-for-size fatty graft repair may be worthwhile to be exploited in future studies. Meanwhile, in this study we observed the mRNA level of notch 4 in oval cell line was also increased during EMT though the result didn't reach statistical significance. Since notch 4 was reported to play a role in tumor EMT [34], we're interested in assessing notch 4 expression at both mRNA and protein levels in the animal model and human specimens in the future.

In summary, with a rat model closely replicating marginal liver graft injury in human, we presented evidence that post-transplant fibrogenesis in small-for-size fatty graft is a dysregulated process involving distinct mechanisms. It was characterized by Aldose reductase activation, oval cell initiation/biliary differentiation/mesenchymal transition as well as notch signaling activation. This indicates that an integrated anti-fibrotic strategy which simultaneously target these key drivers or mediators will probably emerge as a more efficient way to combat post-transplant fibrotic development in human liver transplantation using marginal grafts. Meanwhile, since our study incorporated association study in animal model, validation in human biopsy samples as well as mechanistic exploration in cells, the findings are more feasible to be applied in devising novel therapeutics to achieve maximal benefits for patients receiving liver transplantation.

Abbreviations

AR, aldose reductase; LDLT, living donor liver transplantation; I/R, ischemia/reperfusion; EMT, Epithelial-to-Mesenchymal transition; DR, ductular reaction; TEM, transmitting electron microscopy; MMP14 (MT1-MMP), matrix metallopeptidase 14; ARPC2, actin related protein 2/3 complex subunit 2; MMP9, matrix metallopeptidase 9; DBZ, dibenzazepine; ECM, extracellular matrix; HSCs, hepatic stellate cells.

Supplementary Material

Supplementary figures and tables.
http://www.thno.org/v07p4879s1.pdf

Competing Interests

The authors have declared that no competing interest exists.

References

1. Peeters PM, Sieders E, vd Heuvel M, Bijleveld CM, de Jong KP, TenVergert EM, Slooff MJ, Gouw AS. Predictive factors for portal fibrosis in pediatric liver transplant recipients. *Transplantation*. 2000;70: 1581-7.
2. Imber CJ, St Peter SD, Handa A, Friend PJ. Hepatic steatosis and its relationship to transplantation. *Liver Transpl*. 2002;8: 415-23.
3. Man K, Lo CM, Ng IO, Wong YC, Qin LF, Fan ST, Wong J. Liver transplantation in rats using small-for-size grafts: a study of hemodynamic and morphological changes. *Arch Surg*. 2001;136: 280-5.
4. Cheng Q, Ng KT, Fan ST, Lim ZX, Guo DY, Liu XB, Liu Y, Poon RT, Lo CM, Man K. Distinct mechanism of small-for-size fatty liver graft injury--Wnt4 signaling activates hepatic stellate cells. *Am J Transplant*. 2010;10: 1178-88.
5. Beckebaum S, Iacob S, Klein CG, Dechene A, Varghese J, Baba HA, Sotiropoulos GC, Paul A, Gerken G, Cicinnati VR. Assessment of allograft fibrosis by transient elastography and noninvasive biomarker scoring systems in liver transplant patients. *Transplantation*. 2010;89: 983-93.
6. Bhat M, Ghali P, Rollet-Kurhajec KC, Bhat A, Wong P, Deschenes M, Sebastiani G. Serum fibrosis biomarkers predict death and graft loss in liver transplant recipients. *Liver Transpl*. 2015;21: 1383-94.
7. Omenetti A, Porrello A, Jung Y, Yang L, Popov Y, Choi SS, Witek RP, Alpini G, Venter J, Vandongen HM, Syn WK, Baroni GS, et al. Hedgehog signaling regulates epithelial-mesenchymal transition during biliary fibrosis in rodents and humans. *J Clin Invest*. 2008;118: 3331-42.
8. Knight B, Akhurst B, Matthews VB, Ruddell RG, Ramm GA, Abraham LJ, Olynyk JK, Yeoh GC. Attenuated liver progenitor (oval) cell and fibrogenic responses to the choline deficient, ethionine supplemented diet in the BALB/c inbred strain of mice. *J Hepatol*. 2007;46: 134-41.
9. Robertson H, Kirby JA, Yip WW, Jones DE, Burt AD. Biliary epithelial-mesenchymal transition in posttransplantation recurrence of primary biliary cirrhosis. *Hepatology*. 2007;45: 977-81.
10. Zeisberg M, Yang C, Martino M, Duncan MB, Rieder F, Tanjore H, Kalluri R. Fibroblasts derive from hepatocytes in liver fibrosis via epithelial to mesenchymal transition. *J Biol Chem*. 2007;282: 23337-47.
11. Kupiec-Weglinski J, Busuttil R: Ischemia and reperfusion injury in liver transplantation. *Transplant Proc* 2005; 37:1653-6.
12. Li CX, Ng KT, Shao Y, Liu XB, Ling CC, Ma YY, Geng W, Qi X, Cheng Q, Chung SK, Lo CM, Man K. The Inhibition of Aldose Reductase Attenuates Hepatic Ischemia-Reperfusion Injury Through Reducing Inflammatory Response. *Ann Surg*. 2014;260: 317-28.
13. Chen T, Shi D, Chen J, Yang Y, Qiu M, Wang W, Qiu L. Inhibition of aldose reductase ameliorates diet-induced nonalcoholic steatohepatitis in mice via modulating the phosphorylation of hepatic peroxisome proliferator-activated receptor α. *Mol Med Rep* 2015;11: 303-8.
14. Harada K, Sato Y, Ikeda H, Isse K, Ozaki S, Enomae M, Ohama K, Katayanagi K, Kurumaya H, Matsui A, Nakanuma Y. Epithelial-mesenchymal transition induced by biliary innate immunity contributes to the sclerosing cholangiopathy of biliary atresia. *J Pathol*. 2009;217: 654-64.
15. Choi SS, Diehl AM. Epithelial-to-mesenchymal transitions in the liver. *Hepatology*. 2009;50: 2007-13.
16. Rygiel KA, Robertson H, Marshall HL, Pekalski M, Zhao L, Booth TA, Jones DE, Burt AD, Kirby JA. Epithelial-mesenchymal transition contributes to

portal tract fibrogenesis during human chronic liver disease. *Lab Invest*. 2008;88: 112-23.

17. Scholten D, Osterreicher CH, Scholten A, Iwaisako K, Gu G, Brenner DA, Kisseleva T. Genetic labeling does not detect epithelial-to-mesenchymal transition of cholangiocytes in liver fibrosis in mice. *Gastroenterology*. 2010;139: 987-98.

18. Chu AS, Diaz R, Hui JJ, Yanger K, Zong Y, Alpini G, Stanger BZ, Wells RG. Lineage tracing demonstrates no evidence of cholangiocyte epithelial-to-mesenchymal transition in murine models of hepatic fibrosis. *Hepatol*. 2011;53: 1685-95.

19. Xie G, Diehl AM. Evidence for and against epithelial-to-mesenchymal transition in the liver. *Am J Physiol Gastrointest Liver Physiol*. 2013;305: G881-90.

20. Ling CC, Ng KT, Shao Y, Geng W, Xiao JW, Liu H, Li CX, Liu XB, Ma YY, Yeung WH, Qi X, Yu J, et al. Post-transplant endothelial progenitor cell mobilization via CXCL10/CXCR3 signaling promotes liver tumor growth. *J Hepatol*. 2014;60: 103-9.

21. Ueberham E, Aigner T, Ueberham U, Gebhardt R. E-cadherin as a reliable cell surface marker for the identification of liver specific stem cells. *J Mol Histol*. 2007;38: 359-68.

22. Okabe M, Tsukahara Y, Tanaka M, Suzuki K, Saito S, Kamiya Y, Tsujimura T, Nakamura K, Miyajima A. Potential hepatic stem cells reside in EpCAM+ cells of normal and injured mouse liver. *Development*. 2009;136: 1951-60.

23. Tammali R, Ramana KV, Srivastava SK. Aldose reductase regulates TNF-alpha-induced PGE2 production in human colon cancer cells. *Cancer Lett*. 2007;252: 299-306.

24. Varon C, Tatin F, Moreau V, Van Obberghen-Schilling E, Fernandez-Sauze S, Reuzeau E, Kramer I, Genot E. Transforming growth factor beta induces rosettes of podosomes in primary aortic endothelial cells. *Mol Cell Biol*. 2006;26: 3582-94.

25. Schachtner H, Calaminus SD, Thomas SG, Machesky LM. Podosomes in adhesion, migration, mechanosensing and matrix remodeling. *Cytoskeleton (Hoboken)*. 2013;70: 572-89.

26. Murphy DA, Courtneidge SA. The 'ins' and 'outs' of podosomes and invadopodia: characteristics, formation and function. *Nat Rev Mol Cell Biol*. 2011;12: 413-26.

27. Rottiers P, Saltel F, Daubon T, Chaigne-Delalande B, Tridon V, Billottet C, Reuzeau E, Genot E. TGFbeta-induced endothelial podosomes mediate basement membrane collagen degradation in arterial vessels. *J Cell Sci*. 2009;122: 4311-8.

28. Gawden-Bone C, Zhou Z, King E, Prescott A, Watts C, Lucocq J. Dendritic cell podosomes are protrusive and invade the extracellular matrix using metalloproteinase MMP-14. *J Cell Sci*. 2010;123: 1427-37.

29. Lee H, Overall CM, McCulloch CA, Sodek J. A critical role for the membrane-type 1 matrix metalloproteinase in collagen phagocytosis. *Mol Biol Cell*. 2006;17: 4812-26.

30. Welch MD. Cell migration, freshly squeezed. *Cell*. 2015;160: 581-2.

31. Paluch EK, Raz E. The role and regulation of blebs in cell migration. *Curr Opin Cell Biol*. 2013;25: 582-90.

32. Bergert M, Chandradoss SD, Desai RA, Paluch E. Cell mechanics control rapid transitions between blebs and lamellipodia during migration. *Proc Natl Acad Sci U S A*. 2012;109: 14434-9.

33. Chen Y, Zheng S, Qi D, Zheng S, Guo J, Zhang S, Weng Z. Inhibition of Notch signaling by a gamma-secretase inhibitor attenuates hepatic fibrosis in rats. *PLoS One*. 2012;7: e46512.

34. Lombardo Y, Faronato M, Filipovic A, Vircillo V, Magnani L, Coombes RC. Nicastrin and Notch4 drive endocrine therapy resistance and epithelial to mesenchymal transition in MCF7 breast cancer cells. *Breast Cancer Res*. 2014;16: R62.